International Journal of Mass Spectrometry 277 (2008) 84–90

Contents lists available at ScienceDirect

International Journal of Mass Spectrometry

journal homepage: www.elsevier.com/locate/ijms

# Electron ionization of $H_2O$

Simon J. King, Stephen D. Price*

*Department of Chemistry, University College London, 20 Gordon Street, London WC1H 0AJ, UK*

ARTICLE INFO

*Article history:*
Received 28 March 2008
Received in revised form 4 June 2008
Accepted 9 June 2008
Available online 18 June 2008

*Keywords:*
Electron ionization
Partial ionization cross-sections
Ion–ion coincidence
$H_2O$
Water dication

ABSTRACT

Relative partial ionization cross-sections and precursor-specific relative partial ionization cross-sections for fragment ions formed by electron ionization of $H_2O$ have been measured using time-of-flight mass spectrometry coupled with a 2D ion coincidence technique. We report data for the formation of $H^+$, $H_2^+$, $O^{2+}$, $O^+$ and $OH^+$ relative to the formation of $H_2O^+$, as a function of ionizing electron energy from 30 to 200 eV. This data includes, for the first time, measurements on the formation all positive ion pairs and ion triples by dissociative multiple electron ionization of $H_2O$. Through determinations of the kinetic energy release involved in ion pair formation we provide further evidence that indirect processes contribute significantly to the yield of $H^+ + OH^+$ ion pairs below the vertical double ionization threshold.



## 1. Introduction

Ionization of $H_2O$ is a process of importance in planetary atmospheres [1] and comets [2]. In addition, the emission of slow secondary electrons following dissociative ionization of water present in biological tissue plays a crucial role in DNA damage following radiolysis [3]. A detailed understanding of these processes requires, among other factors, accurate and reliable data on the partial ionization cross-sections (PICS) for forming both the parent ion and the various ionic fragments resulting from single and multiple ionization [4].

The PICS following electron ionization of water vapour have been the subject of a number of previous experimental investigations. Schutten et al. [5] measured PICS for the formation of all singly and doubly charged ions in the energy range 20–2000 eV and PICS for the formation of $H_2O^+$, $OH^+$, $O^+$ and $H^+$ have been measured using a quadrupole mass spectrometer (QMS) by Orient and Srivastava [6], up to an ionizing energy of 400 eV. Rao et al. [7] used a QMS with an improved ion extraction technique to measure PICS for the formation of ions with up to 5 eV of translational energy, at ionizing energies below 1000 eV. Interestingly, Rao et al. [7] reported the direct observation of $H_2O^{2+}$ ions in their mass spectra, although this assignment has recently been questioned [8]. Straub et al. [8] measured PICS for the formation of singly and doubly charged ions for both $H_2O$ and $D_2O$ up to 1000 eV, using a time-of-flight mass spectrometer coupled with position sensitive detection. In this way Straub et al. [8] were able to demonstrate the complete collection of all ionic fragments, including those formed with considerable translational kinetic energy. However, despite the wealth of available experimental data concerning the PICS of water vapour, very few studies have investigated the multiple ionization of $H_2O$ following electron impact. Specifically, Frémont et al. [9] measured the fragment energy distributions of ions formed by single, double and triple ionization, in the ionizing energy range 20–200 eV. Most recently, Montenegro et al. [10] measured cross-sections for the formation of $H^+ + O^+$ and $H^+ + OH^+$ ion pairs, in addition to all single ions, at electron energies between 45 and 1500 eV. To date, complete sets of measurements on the formation of ion pairs and ion triples, following dissociative multiple ionization of $H_2O$, are confined to studies involving collisions with fast ions [11,12].

In this study we investigate the electron ionization of $H_2O$ in the energy range 30–200 eV, using time-of-flight mass spectrometry coupled with a 2D ion coincidence technique. By this method single product ions, ion pairs and ion triples, formed following electron ionization of $H_2O$ are detected concomitantly, then identified and quantified. We report relative PICS $\sigma_r[X^{m+}]$ for the formation of $H^+$, $H_2^+$, $O^{2+}$, $O^+$, and $OH^+$ ions, expressed relative to the formation of $H_2O^+$, as a function of ionizing electron energy in the range 30–200 eV. This data is shown to be in excellent agreement with the existing PICS of Straub et al. [8]. We also present precursor-specific relative PICS $\sigma_n[X^{m+}]$, which, as shown by our recent studies of the electron ionization of $C_2H_2$ [4] and $CO_2$ [13], quantify the contributions to the PICS for a given fragment ion $X^{m+}$ (e.g., $OH^+$) from different levels of ionization: single ($n = 1$), double ($n = 2$) and triple ($n = 3$). Specifically, $\sigma_1[OH^+]$ quantifies the yield of $OH^+$ ions formed *via* single ionization; that is from the initial formation of $H_2O^+$

* Corresponding author. Tel.: +44 20 7679 4606; fax: +44 20 7679 7463.
*E-mail address:* S.D.Price@ucl.ac.uk (S.D. Price).

1387-3806/$ – see front matter © 2008 Elsevier B.V. All rights reserved.
doi:10.1016/j.ijms.2008.06.004

in the electron–molecule collision and the subsequent fragmentation of this primary molecular ion. Similarly $\sigma_2[OH^+]$ quantifies the yield of $OH^+$ ions formed *via* double ionization; that is from the initial formation of $H_2O^{2+}$ in the electron–molecule collision and the subsequent fragmentation of this primary dication. To the best of our knowledge these measurements represent the first complete description of the single and multiple ionization of $H_2O$ by electrons.

Our 2D ion coincidence technique also provides information on the energetics of the dissociation of the $H_2O$ dication. The energies of the electronic states of $H_2O^{2+}$ have been studied using a variety of techniques, including photoion–photoion coincidence (PIPICO) spectroscopy [14,15], photoelectron–photoelectron coincidence (PEPECO) spectroscopy [16], double charge transfer (DCT) spectroscopy [17], Auger electron spectroscopy (AES) [18], and theoretical methods [19–21]. In this study we report measurements of the kinetic energy release (KER) involved in ion pair formation following dissociative double ionization of $H_2O$. These measurements provide further evidence that the formation of $H^+ + OH^+$ ion pairs proceeds *via* indirect processes below the vertical double ionization potential [16].

## 2. Experimental

### 2.1. Experimental apparatus

All experiments in this study were performed using a TOFMS of Wiley–McLaren design, as has been described in detail in recent publications [4,22]. Distilled water which was thoroughly degassed prior to the experiment *via* a sequence of freeze–thaw cycles, was held at a temperature of 273 K using a water-ice bath. The vapour above this sample was introduced to the apparatus *via* a hypodermic needle to form a continuous effusive beam of $H_2O$ in the source region. Electron ionization of this target beam was performed by a pulsed beam of ionizing electrons with duration of 30 ns per pulse and a repetition rate of 50 kHz. We estimate that the energy resolution of the electron beam is 0.5 eV at full width at half maximum. Ion signals from a microchannel plate (MCP) detector were recorded as arrival times by a time-to-digital converter (TDC) capable of recording multiple stop signals per ionizing pulse. The arrival times of ions as single ion detections, or as ion pairs or ion triples, are accumulated in a memory module and transferred periodically to a PC.

### 2.2. Experimental conditions

The operating conditions of our experiment involve low electron flux and low target gas pressures, typically $<10^{-6}$ Torr, ensuring that on average much less than one ionization event occurs per pulse of ionizing electrons. This methodology greatly reduces the number of 'false coincidences' that contribute to our ion coincidence mass spectra. False coincidences arise where two or more ions formed by independent ionization events are detected following a single ionizing pulse. In extracting quantitive data from our experiment we must ensure that all ions are detected with an equal efficiency, regardless of their mass or initial kinetic energy. In a recent publication [4] we described a number of preliminary experiments performed using our apparatus which enabled us to establish a range of voltage conditions whereby mass-dependent and energy-dependent discrimination effects do not influence the ion yields we measure. Under these voltage conditions we found that all ions may reach the detector provided they have a translational energy component of less than 11 eV perpendicular to the TOF axis. Curtis and Eland [23] determined the total KER from the dissociation of small molecular dications to be, commonly, less than 9 eV. Thus, in our experiment, conditions are optimised for the majority of all ions formed by multiple ionization to be collected and indeed, as explained below, any small losses of energetic fragment ions from multiple ionization can be quantified and corrected.

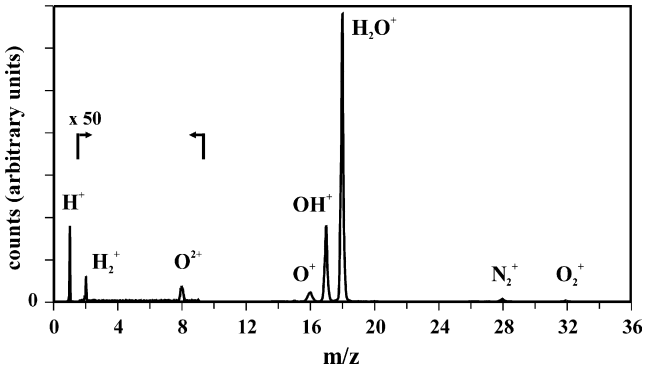


**Fig. 1.** A characteristic (singles) mass spectrum of $H_2O$ following electron impact ionization at 200 eV.

### 2.3. Data processing

Single ion detections following a single ionizing pulse of electrons are termed 'singles' and are accumulated as a histogram of ion counts against time-of-flight to form a 'singles' mass spectrum, as shown in Fig. 1. The mass scale of the mass spectrum is calibrated by recording the mass spectrum of a reference species (Ar) under the same voltage conditions. The intensities of individual ion peaks in the mass spectrum are then extracted by summing the counts in each peak after applying a small correction to account for the non-zero baseline due to background counts. A further correction was made to the intensity of $O^+$ ions and $O^{2+}$ ions measured in each mass spectrum to account for contributions from the ionization of background $O_2$ gas present in our vacuum chamber, using a procedure described in our recent study on $CO_2$ [13]. Typically contributions to the raw $O^+$ peak intensity from the background gas are much less than 2%.

Events resulting in the detection of two ions and three ions following a single ionizing pulse of electrons, termed 'pairs' and 'triples', respectively, are stored and processed offline. Ion pairs are plotted as a 2D histogram of the respective ion flight times ($t_1$ vs. $t_2$), termed a 'pairs' spectrum. The contribution of a fragment ion to the pairs spectrum is obtained by summing the intensity of all the appropriate spectral peaks. Since we show below that the contribution of quadruple ionization can be neglected in this study, some ion pairs can only be formed *via* dissociative triple ionization ($H^+ + O^{2+}$) and some ion pairs may have contributions from both double and triple ionization ($H^+ + O^+$). Contributions from triple ionization to the intensities of such monocation pairs may arise when only two ions of an ion triple are detected, due to the less than unit collection efficiency of the apparatus.

All peaks within our pairs spectra contain a small number of additional counts due to false coincidences, although such contributions are minimised experimentally by operating at low ion count rates. The number of false coincidences is evaluated manually for each peak using an ion-autocorrelation function [4] and then subtracted; false coincidences typically account for 1–2% of the raw peak intensities at higher ionizing electron energy, In our experiment no ion pairs are recorded if the second ion arrives at the detector within 32 ns of the first ion, due to the 'deadtime' of the discrimination circuitry. Such deadtime losses significantly affect the number of counts recorded in the $H^+ + H^+$ peak in our pairs spectra.

To estimate the number of ions lost, a separate one-dimensional $(t_2 - t_1)$ spectrum is constructed from the $H^+ + H^+$ coincidence data which is then appropriately extrapolated to the limit $t_1 = t_2$ to correct for the losses.

As described above, ions may reach the detector provided they have a translational energy component of less than 11 eV perpendicular to the TOF axis. However, if the total KER involved in ion pair formation exceeds this value, a small proportion of ions forming coincident ion pairs may be 'missed'. Any such losses most commonly arise for ion pairs comprising $H^+$ in coincidence with an ion of greater mass, since conservation of linear momentum dictates that most of the energy released in the dissociation process is partitioned to the lighter $H^+$ ion. These losses are evidenced by a small hollowing of the corresponding $(t_2 - t_1)$ plot for a particular ion peak, as has been demonstrated in previous PIPICO studies. In this study we observe small losses of energetic $H^+ + O^+$ ion pairs at ionizing energies above 100 eV, which we again evaluate in each pairs spectrum as discussed above [24]. The size of this correction does not exceed 10% of the raw $H^+ + O^+$ pairs peak intensity in the ionizing energy range investigated in this study. We note however that we are unable to correct for any losses of energetic monocations from single ionization, or dications from double ionization, if such fragment ions are formed with a kinetic energy greater than 11 eV.

Ion triples are processed by specifying a time-of-flight range for a particular ion ($O^+$), and then extracting all ion triples containing at least one ion whose arrival time $t_1$ lies within this specified range. Once extracted, the respective flight times of the two remaining ions ($H^+ + H^+$) forming an ion triple are plotted as a 2D histogram ($t_2$ vs. $t_3$). The contribution of a fragment ion to the triples spectrum is then obtained from the number of counts in this $H^+ + H^+$ peak, after applying a small geometric correction to account for losses due to the 'deadtime', as described above. We consider only the formation of $H^+ + H^+ + O^{q+}$ ion triples *via* dissociative triple ionization ($q = 1$), since the number of ion triples detected for quadruple or higher order ionization ($q \geq 2$) are too small to be quantified over the range of ionizing energies investigated. False triple coincidences that contribute to the $H^+ + H^+ + O^+$ counts are subtracted using a procedure outlined in a recent publication [4]. All ion intensities measured in this work were corrected numerically using the natural isotopic distributions.

### 2.4. Data reduction

The ion intensities measured in our spectra are processed to yield relative PICS and precursor-specific relative PICS. Relative PICS, represented as $\sigma_r[X^+]$ for fragment monocations ($X^+$) and $\sigma_r[X^{2+}]$ for dications ($X^{2+}$), represent the cross-section for forming a particular ionic fragment from all levels of ionization, expressed relative to the cross-section for forming the parent monocation $H_2O^+$. Precursor-specific relative PICS are symbolized by $\sigma_n[X^+]$ and represent the relative cross-section for forming an ion ($X^+$) by single ($n = 1$), double ($n = 2$) or triple ($n = 3$) ionization.

Our aim is to derive $\sigma_r$ values and $\sigma_n$ values for all the ions detected in our experiments. Recently we have reported an algorithm to show that $\sigma_r$ can be expressed in terms of the ion intensities recorded in our singles, pairs and triples spectra [4]. Similarly we have shown that precursor-specific relative PICS $\sigma_n$ can be expressed in terms of the spectral intensities and the ion detection efficiency $f_i$. The ion detection efficiency must be considered to account for the transmission efficiency of the grids that define the electric fields in our apparatus, and also the efficiency of the detector and electronics. For a full description of the data reduction procedure used for the derivation of these cross-sections the reader is referred to Ref. [4]. To measure the ion detection efficiency $f_i$ separate experiments were performed, under the same voltage conditions employed in this study, to record the intensity of single ions and ion pairs formed by electron ionization of $CF_4$. Comparison of this data to the corresponding absolute measurements of Bruce and Bonham [25,26] yields a value of $f_i$, as has been described previously in the literature [4,13,22,24].

**Table 1**
Relative partial ionization cross-sections following electron ionization of $H_2O$, expressed relative to the cross-section for forming $H_2O^+$, as a function of electron energy $E$

| $E$ (eV) | $\sigma_r[H^+]$ | $10^2\ \sigma_r[H_2^+]$ | $10^2\ \sigma_r[O^{2+}]$ | $\sigma_r[O^+]$ | $\sigma_r[OH^+]$ |
|---|---|---|---|---|---|
| 200 | 0.261 (11) | 0.118 (6) | 0.173 (30) | 0.0671 (18) | 0.315 (3) |
| 175 | 0.263 (9) | 0.119 (18) | 0.149 (20) | 0.0667 (14) | 0.315 (1) |
| 150 | 0.261 (12) | 0.117 (10) | 0.109 (11) | 0.0651 (18) | 0.313 (3) |
| 125 | 0.255 (12) | 0.116 (11) | 0.067 (17) | 0.0615 (15) | 0.310 (2) |
| 100 | 0.240 (11) | 0.113 (8) | 0.024 (3) | 0.0540 (13) | 0.305 (3) |
| 85 | 0.225 (12) | 0.112 (5) | 0.005 (3) | 0.0466 (17) | 0.299 (2) |
| 75 | 0.209 (9) | 0.113 (12) | 0.000 (3) | 0.0402 (15) | 0.293 (3) |
| 65 | 0.185 (8) | 0.109 (8) | 0.001 (1) | 0.0328 (11) | 0.285 (2) |
| 60 | 0.174 (8) | 0.109 (16) | 0.000 (1) | 0.0292 (18) | 0.279 (2) |
| 55 | 0.160 (8) | 0.107 (12) | 0.000 (1) | 0.0255 (16) | 0.273 (2) |
| 50 | 0.141 (8) | 0.107 (12) | 0.000 (1) | 0.0202 (11) | 0.262 (2) |
| 45 | 0.124 (7) | 0.109 (8) | 0.000 (1) | 0.0159 (10) | 0.252 (4) |
| 40 | 0.109 (6) | 0.104 (11) | 0.000 (1) | 0.0101 (25) | 0.239 (5) |
| 35 | 0.089 (6) | 0.096 (12) | 0.000 (1) | 0.0052 (8) | 0.218 (3) |
| 30 | 0.068 (5) | 0.076 (5) | 0.000 (1) | 0.0013 (9) | 0.184 (4) |

The value in parenthesis indicates two standard deviations in the last figure.

### 2.5. Dication energetics $H_2O^{2+}$

The shape of the peaks in the pairs spectrum can be interpreted, by the use of Monte Carlo simulations [4,13], to yield information on the KER upon fragmentation of the water dication $H_2O^{2+}$. Measurement of the KER enables the estimation of the precursor state energy of the water dication, which dissociates to form the ion pair of interest, if the asymptotic energy of the dissociation limit is known or assumed.

## 3. Results

Mass and coincidence spectra of $H_2O$ were recorded at ionizing electron energies in the range 30–200 eV. Relative PICS $\sigma_r$ for the formation of fragment ions ($H^+$, $H_2^+$, $O^{2+}$, $O^+$, and $OH^+$) were derived using the analysis procedure described above, and are displayed in Table 1 and Figs. 2–4, as a function of electron energy. Precursor-specific PICS $\sigma_n$ for the formation of these ions are shown in Table 2 and Figs. 4 and 5. The overall contributions from single, double and triple ionization, as a percentage of the total ion yield at each ionizing electron energy, are summarized in Table 3. Measurements of the ion detection efficiency ($f_i$) for our apparatus, as described in Section 2.4, resulted in a value of $f_i = 0.19 \pm 0.01$, in close agreement with previous determinations [4,13,22].

In our pairs spectra we observe three dissociation channels of $H_2O^{2+}$: $H^+ + OH^+$, $H^+ + O^+ + H$ and $H^+ + H^+ + O$. In addition, at electron energies above 85 eV we observe one ion pair and one ion triple resulting from dissociation of $H_2O^{3+}$: $H^+ + O^{2+} + H$ and $H^+ + H^+ + O^+$. The conclusions drawn from these coincidence signals concerning the energetics of dissociative double ionization of $H_2O^{2+}$ are discussed below.

## 4. Discussion

### 4.1. Relative partial ionization cross-sections

The values of $\sigma_r$ we determine for formation of $H^+$, $H_2^+$, $O^{2+}$, $O^+$ and $OH^+$ ions are shown in Figs. 2 and 3, respectively. Where

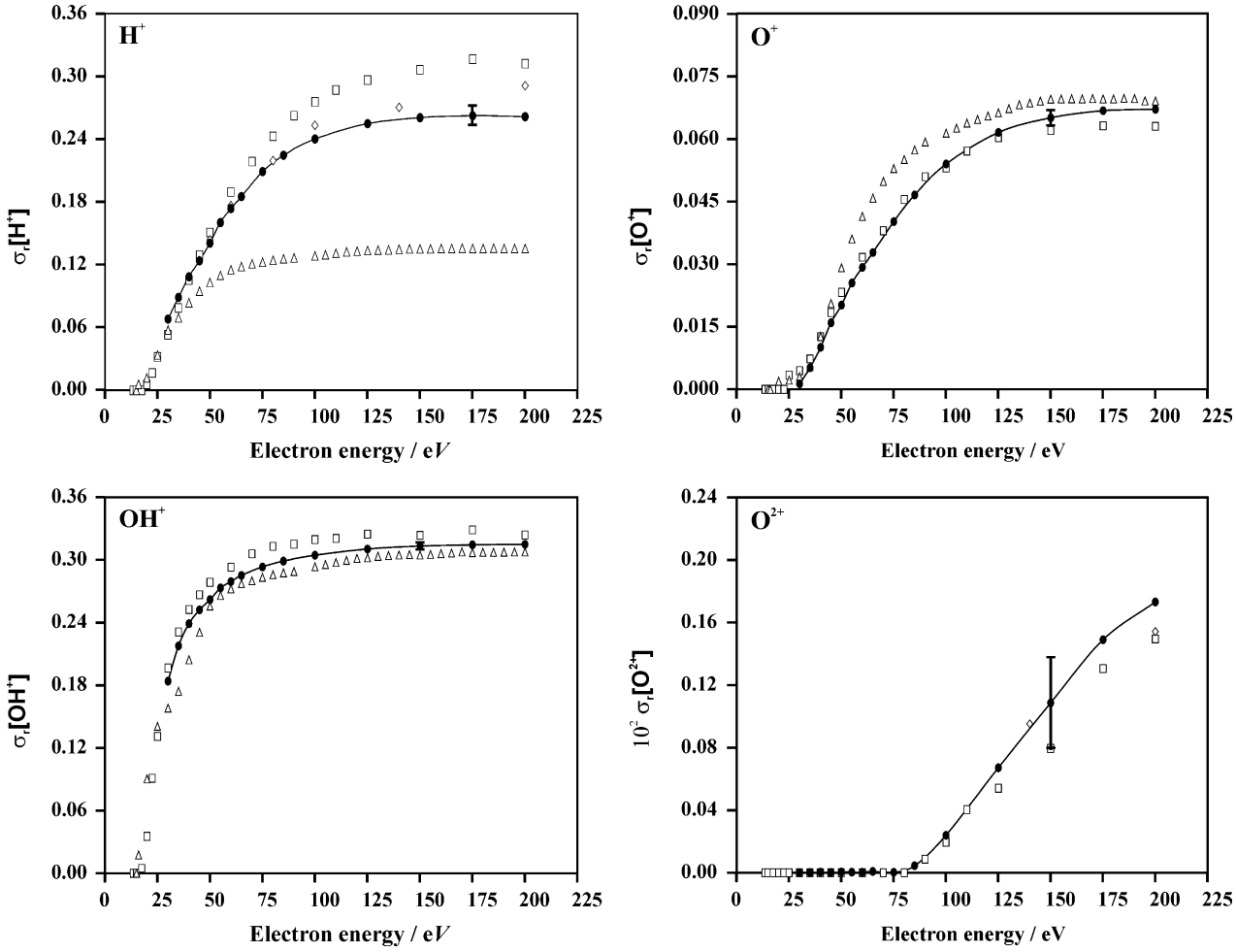


**Fig. 2.** Relative PICS $\sigma_r[X^{n+}]$ for forming fragment ions (●) following electron ionization of $H_2O$. The error bars expressed in this figure represent four standard deviations of four separate determinations. The corresponding relative PICS extracted from the data of Rao et al. (△), Montenegro et al. (◊), and analogous relative PICS extracted from the data of Straub et al. (□), are also shown.

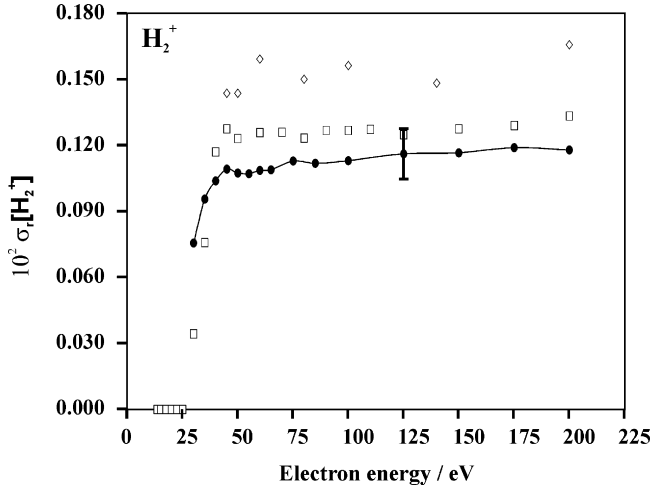


**Fig. 3.** Relative PICS $\sigma_r[X^{n+}]$ for forming $H_2^+$ ions (●) following electron ionization of $H_2O$. The error bars expressed in this figure represent four standard deviations of four separate determinations. The corresponding relative PICS extracted from the data of Montenegro et al. (◊), and analogous relative PICS extracted from the data of Straub et al. (□), are also shown.

appropriate, these values are compared with values of relative PICS derived from the $H_2O$ data of Rao et al. [7] and Montenegro et al. [10], and the $D_2O$ data of Straub et al. [8]. We note here that a direct comparison with the $H_2O$ data of Straub et al. [8] for the formation of $O^+$, $OH^+$ and $H_2O^+$, is not possible as these authors report only combined cross-sections for the formation of these ions. However, Straub et al. [8] deduced from their data that the PICS for forming $O^+$, $OH^+$ and $H_2O^+$ from $H_2O$ were the same, within experimental error, as the PICS for forming $O^+$, $OD^+$ and $D_2O^+$ from $D_2O$. Thus, we compare our $\sigma_r$ values for the formation of $O^+$, $OH^+$ and $H_2O^+$ with the data from Straub et al. [8] for the corresponding ions formed from $D_2O$. For $H^+$ and $H_2^+$ we extract $\sigma_r$ values from the data of Straub et al. [8] by normalizing the PICS for forming $H^+$ and $H_2^+$ to that reported for forming $D_2O^+$. Over the entire ionizing energy range there is excellent agreement between our $\sigma_r[X^+]$ values and these values derived from Straub et al. [8].

A comparison of our $\sigma_r[X^+]$ values to the data of Montenegro et al. [10], not shown for the formation of monocation fragments in Fig. 2 for clarity, similarly reveal an excellent agreement between the two data sets. By contrast, the $\sigma_r[H^+]$ values derived from the data of Rao et al. [7] lie considerably lower than these data sets, and these differences can be explained by the inefficient collection of $H^+$ ions formed with significant translational energy in this earlier work. In our mass spectra we observe no discernible peaks

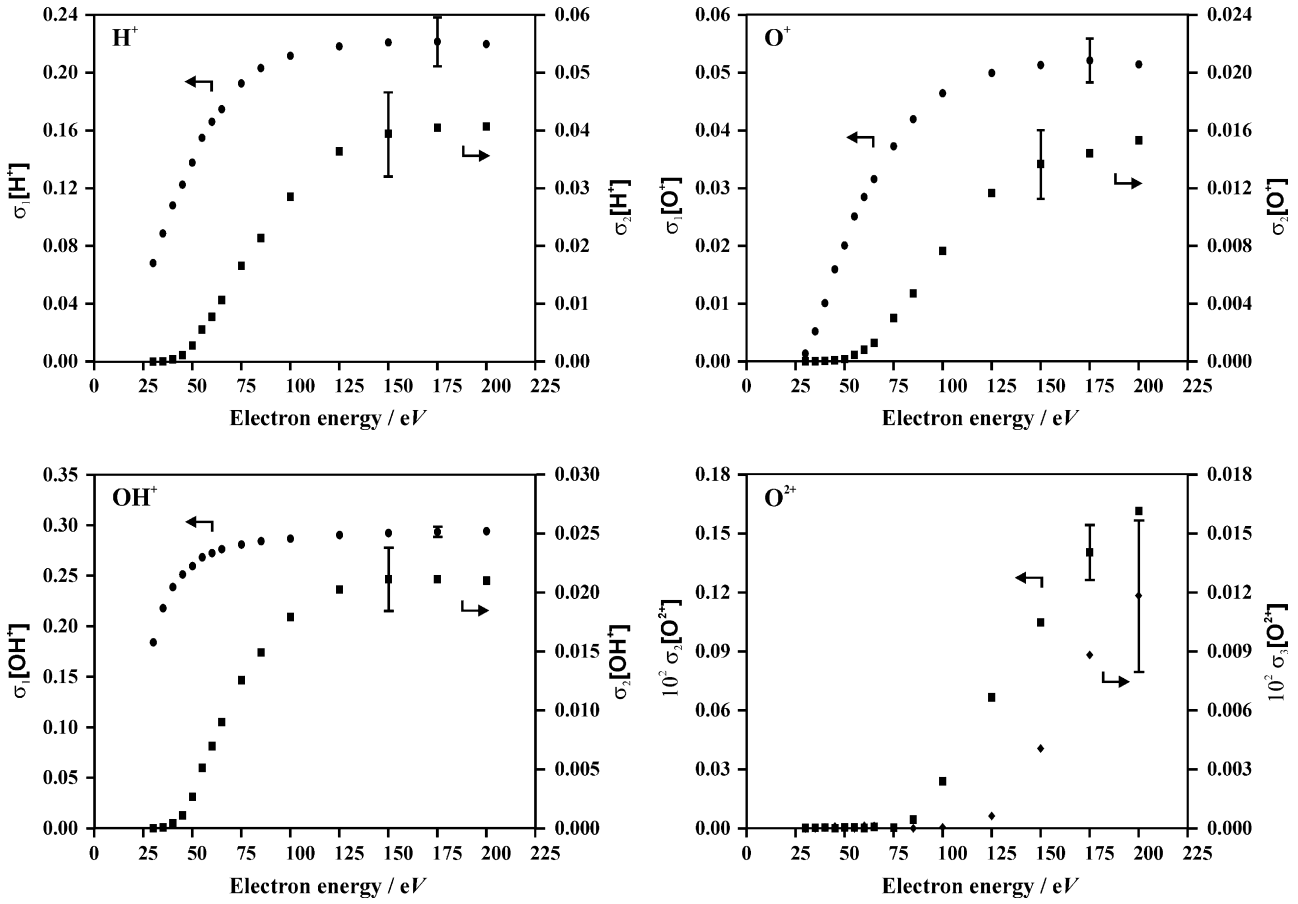


**Fig. 4.** Relative precursor-specific PICS for forming ion fragments *via* single ionization (●), *via* double ionization (■), and *via* triple ionization (♦), following electron ionization of $H_2O$. The representative error bars show four standard deviations of four separate determinations.

attributable to $H_2O^{2+}$ formation and, hence, we place an upper limit of 0.00005 on $\sigma_r[H_2O^{2+}]$ for electrons of energy 30–200 eV.

### 4.2. Relative precursor-specific PICS

Comparison of $\sigma_1[X^+]$ and $\sigma_2[X^+]$ values for the formation of monocation fragments $H^+$, $O^+$ and $OH^+$ (Fig. 4), reveal that contributions to the yields of these ions *via* dissociative double ionization are small compared to contributions from dissociative single ionization. Our data (Fig. 4) also shows that contributions to the $O^{2+}$ ion yield are from both double and triple ionization, although we note that our $\sigma_3[O^{2+}]$ values are an order of magnitude lower than the corresponding $\sigma_2[O^{2+}]$ values. Contributions to the yield of $H^+$ ions and $O^+$ ions *via* dissociative triple ionization (Fig. 5) are similarly at least an order of magnitude smaller than the corresponding $\sigma_2[X^+]$ values. If this minor contribution from triple ionization is neglected, a comparison can be made between our $\sigma_2[O^+]$ and $\sigma_2[OH^+]$ values with the cross-section measurements of Montenegro et al. [10] for forming $H^+ + O^+$ and $H^+ + OH^+$ ion pairs. Such a comparison reveals a less satisfactory agreement between the data sets. For example, at 100 eV our $\sigma_2[O^+]$ and $\sigma_2[OH^+]$ values are both around 40% lower than the corresponding values extracted from the data of Montenegro et al. [10], while at 200 eV these differences are about 50%. The origin of these discrepancies is not readily apparent. In our pairs spectra recorded at 200 eV over a longer time period, we also see evidence of a weak peak corresponding to $H_2^+ + O^+$ formation. Our measurements suggest that the intensity of this minor ion pair peak at 200 eV is only 0.12% of the intensity of the major ion pair peak $H^+ + OH^+$. This value concurs with an upper limit of 0.2% proposed in the PIPICO study of Richardson et al. at 40.8 eV [14].

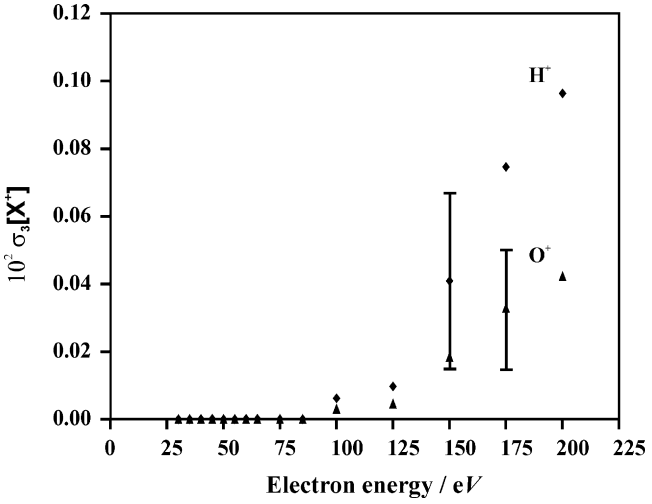


**Fig. 5.** Relative precursor-specific PICS for forming monocation fragments ($H^+$ (♦) and $O^+$ (▲)) *via* triple ionization, following electron ionization of $H_2O$. The representative error bars show four standard deviations of four separate determinations.

In Table 3 we show that contributions to the total ion yield from double ionization increase slowly to 4.8% at 200 eV. This value lies higher than the value of 1% proposed by Frémont et al. [9], based on conclusions drawn from the KER distribution of all ions formed at 200 eV. We can compare the maximum in the ion yield from double ionization yield for $H_2O$ (4.8%) to corresponding yields for

**Table 2**
Relative precursor-specific PICS for forming fragment ions following dissociative electron ionization of $H_2O$, expressed relative to the cross-section for forming $H_2O^+$, as a function of electron energy $E$

| $E$/eV | $\sigma_1[H^+]$ | $\sigma_2[H^+]$ | $10^2\ \sigma_3[H^+]$ | $10^2\ \sigma_2[O^{2+}]$ | $10^2\ \sigma_3[O^{2+}]$ | $\sigma_1[O^+]$ |
|---|---|---|---|---|---|---|
| 200 | 0.220 (19) | 0.0407 (80) | 0.096 (51) | 0.161 (33) | 0.0118 (40) | 0.0514 (50) |
| 175 | 0.221 (17) | 0.0405 (80) | 0.075 (37) | 0.140 (24) | 0.0088 (50) | 0.0520 (38) |
| 150 | 0.221 (19) | 0.0394 (73) | 0.041 (27) | 0.105 (14) | 0.0041 (27) | 0.0512 (40) |
| 125 | 0.218 (18) | 0.0364 (71) | 0.010 (13) | 0.067 (17) | 0.0006 (16) | 0.0499 (28) |
| 100 | 0.211 (17) | 0.0285 (62) | 0.006 (7) | 0.024 (3) | 0.0000 (2) | 0.0464 (23) |
| 85 | 0.203 (16) | 0.0214 (40) | 0.000 (1) | 0.005 (3) | 0.0000 (1) | 0.0419 (22) |
| 75 | 0.192 (13) | 0.0166 (39) | 0.000 (1) | 0.000 (3) | 0.0000 (1) | 0.0372 (18) |
| 65 | 0.175 (10) | 0.0106 (19) | | 0.001 (1) | | 0.0315 (11) |
| 60 | 0.166 (9) | 0.0078 (9) | | 0.000 (1) | | 0.0284 (19) |
| 55 | 0.155 (9) | 0.0056 (8) | | | | 0.0250 (16) |
| 50 | 0.138 (9) | 0.0028 (8) | | | | 0.0200 (11) |
| 45 | 0.122 (7) | 0.0011 (2) | | | | 0.0159 (10) |
| 40 | 0.108 (6) | 0.0004 (3) | | | | 0.0101 (25) |
| 35 | 0.089 (7) | 0.0001 (1) | | | | 0.0052 (8) |
| 30 | 0.068 (5) | 0.0000 (1) | | | | 0.0013 (9) |

| $E$/eV | $\sigma_2[O^+]$ | $10^2\ \sigma_3[O^+]$ | $\sigma_1[OH^+]$ | $\sigma_2[OH^+]$ |
|---|---|---|---|---|
| 200 | 0.0153 (28) | 0.042 (24) | 0.294 (6) | 0.0210 (16) |
| 175 | 0.0144 (24) | 0.033 (18) | 0.293 (5) | 0.0211 (18) |
| 150 | 0.0136 (24) | 0.018 (13) | 0.292 (6) | 0.0211 (13) |
| 125 | 0.0116 (17) | 0.005 (6) | 0.290 (5) | 0.0202 (13) |
| 100 | 0.0076 (12) | 0.003 (4) | 0.287 (5) | 0.0179 (13) |
| 85 | 0.0047 (6) | 0.000 (1) | 0.284 (5) | 0.0149 (14) |
| 75 | 0.0030 (5) | 0.000 (1) | 0.281 (4) | 0.0126 (10) |
| 65 | 0.0013 (1) | | 0.276 (2) | 0.0090 (5) |
| 60 | 0.0008 (1) | | 0.272 (3) | 0.0070 (4) |
| 55 | 0.0004 (1) | | 0.268 (3) | 0.0051 (4) |
| 50 | 0.0001 (1) | | 0.259 (2) | 0.0027 (4) |
| 45 | 0.0001 (1) | | 0.251 (4) | 0.0011 (1) |
| 40 | 0.0000 (1) | | 0.239 (5) | 0.0004 (1) |
| 35 | 0.0000 (1) | | 0.218 (4) | 0.0001 (1) |
| 30 | 0.0000 (1) | | 0.184 (4) | 0.0000 (1) |

The value in parenthesis indicates two standard deviations in the last figure.

other small molecules $C_2H_2$ (11%) [4], HCl (11%) [24], $CH_4$ (12%) and $CO_2$ (17%) [13]. This comparison shows that in the ionizing electron energy range 30–200 eV the yield of dissociative double ionization for $H_2O$ is low. Indeed, a low quantum yield for double ionization for $H_2O$ has been reported previously by Eland [16] using TOF-PEPECO measurements. Recent theoretical work on the water dication $H_2O^{2+}$ [20] indicated the potential curves for a number of low-lying dication states were almost 'flat' over a range of internuclear distances. Such "flat" potential energy surfaces may delay the dissociation of $H_2O^{2+}$, but, of course, they cannot account for a low yield of dissociative double ionization if we do not observe long-lived dications experimentally. Hence, it seems clear that, in the experimental energy regime, the intrinsic probability for removing two electrons from $H_2O$ is small, perhaps due to some underlying feature of the electron-correlation in the molecule.

**Table 3**
Contributions to the total ion yield from single, double and triple ionization, following electron ionization of $H_2O$, as a function of electron energy $E$

| $E$ (eV) | Single ionization (%) (3SF) | Double ionization (%) (1DP) | Triple ionization (%) (1SF) |
|---|---|---|---|
| 200 | 95.1 | 4.8 | 0.09 |
| 175 | 95.2 | 4.7 | 0.07 |
| 150 | 95.4 | 4.6 | 0.04 |
| 125 | 95.8 | 4.2 | 0.01 |
| 100 | 96.6 | 3.4 | 0.01 |
| 85 | 97.4 | 2.6 | 0 |
| 75 | 97.9 | 2.1 | 0 |
| 65 | 98.6 | 1.4 | 0 |
| 60 | 99.0 | 1.1 | 0 |
| 55 | 99.2 | 0.8 | 0 |
| 50 | 99.6 | 0.4 | 0 |
| 45 | 99.8 | 0.2 | 0 |
| 40 | 99.9 | 0.1 | 0 |
| 35 | 99.9. | 0.1 | 0 |
| 30 | 100 | 0.0 | 0 |

### 4.3. The energetics of dissociative double ionization

The kinetic energy of the ion pairs formed by dissociation of the $H_2O^{2+}$ dication have been determined using Monte Carlo simulations of the peaks we observe in the pairs spectrum, as described in Section 2.5. KER determinations for the formation of $H^+ + OH^+$ and $H^+ + O^+$ ion pairs were made from data recorded at electron energies above 50 and 75 eV, respectively, as the coincidence spectra recorded at electron energies lower than these values contained insufficient coincidence signals to produce statistically significant results. In these simulations all KER components were modelled using a Gaussian distribution with a width of 1.2 eV at FWHM, the minimum width which gives a satisfactory fit to releases which clearly appear single valued. Indeed, such simulated KER distributions yield KER values in excellent agreement with literature values for different molecules. [4,13,27–29]. In the sections that follow here we compare our KER measurements with other available experimental data.

#### 4.3.1. $H^+ + OH^+$

The formation of $H^+ + OH^+$ ion pairs is the dominant dication dissociation channel at all the ionizing energies investigated in this study. For this ion pair at 50 eV we determine two KER components with a near equal weighting, the first centred at $3.6 \pm 0.4$ eV and a second larger KER of $9.2 \pm 0.5$ eV, suggesting an average KER of around $6.4 \pm 0.5$ eV. This smaller KER component rises steadily to a value of $5.2 \pm 0.4$ eV above 75 eV, while the second KER component

remains as 9.2 eV with an increased weighting of 60%. Our values of the KER in the ionizing energy range 50–75 eV agree only partially with corresponding data from earlier PIPICO measurements of Richardson et al. [14], who determined an average KER of 4.5 ± 0.5 eV at a photon energy of 40.8 eV. In a separate PIPICO study, Winkoun et al. [15] observed two KER components for $H^+ + OH^+$ formation at 41 eV, 3.0 ± 0.3 and 5.5 ± 0.5 eV respectively. Of these values, only the smaller component of KER agrees with our observations, within experimental error, at ionizing electron energy of 50 eV.

Our KER of 3.6 ± 0.4 eV obtained at 50 eV suggests a dissociative precursor state lying at 35.4 ± 0.4 eV, assuming the formation of ground state products $H^+ + OH^+ (^3\Sigma^-)$, a dissociation limit which lies at 31.78 eV [30,31] with respect to the ground state of $H_2O$. This value lies considerably lower than measurements of the vertical double ionization energy 39.6 eV, obtained by double charge transfer experiments [17]. Thus, our data provides additional evidence for the formation of $H^+ + OH^+$ ion pairs *via* an indirect two-step process, involving an autoionization step well outside of the vertical Franck–Condon region, as shown in the recent PEPECO study [16] A similar indirect double ionization mechanism has recently been observed for $CO_2$ [13,32].

Previous work using our apparatus has demonstrated that we measure reliable KER values for dicationic dissociation processes, which form an $H^+$ ion [4]. Thus, the discrepancy between our KER values and those from the photoionization studies is most likely due to higher energy dication states being accessed in our experiments using 50 eV electrons than with the lower energy photons.

#### 4.3.2. $H^+ + O^+ + H$

From a Monte Carlo simulation of the coincidence data for $H^+ + O^+ + H$ formation at 75 eV we determine a single-valued KER of 11.5 ± 0.5 eV. In addition, at ionizing electron energies in excess of 75 eV we observe the growth of a second single-valued KER component of around 17 eV. These simulations assume that this ion pair is formed *via* a concerted mechanism [33], although we note here that additional simulations performed assuming a two-step dissociation process yield nearly identical energy releases. Furthermore, these determinations of the KER represent a lower limit for the total KER release involved in $H^+ + O^+ + H$ formation, as a small additional amount of translational energy may be partitioned to the neutral H atom that is not detected by our apparatus. The corresponding photoionization measurements of Richardson et al. [14] (5 ± 0.5 eV) at 41.8 eV, and Winkoun et al. [15] (4.7 ± 0.3 eV) (46 eV), obtained from PIPICO measurements significantly closer to the double ionization threshold, are considerably smaller than the KER values we determine for $H^+ + O^+ + H$ formation with 75 eV electrons. Again, a likely explanation for this discrepancy is that our experiments are dominated by the dissociation of excited dication states lying high in the electronic state manifold of $H_2O^{2+}$, which were not accessed in the earlier photoionization experiments. The identity of these excited states is unknown, as the electronic structure of the water dication high above the double ionization potential has not been investigated.

## 5. Conclusion

Time-of-flight mass spectrometry coupled with a 2D ion coincidence technique has been used to measure relative PICSs for the formation of positively charged ions following electron ionization of $H_2O$ in the energy range 30–200 eV. Using this methodology we have also derived relative precursor-specific PICS, which enable us to quantify the contribution to the yield of each fragment ion from single, double and triple ionization. These measurements include, for the first time, contributions from all positive ion pairs and ion triples formed by dissociative electron ionization.

Excellent agreement is found between our data and a recent determination of the PICS of $H_2O$, in which the efficient collection of all ion fragments with considerable translational energy was demonstrated. Our precursor-specific PICS reveal that contributions to the yield of all fragment monocations are dominated by single ionization up to ionizing electron energy of 200 eV. In this ionizing energy regime, the overall contributions from dissociative double ionization to the total ion yield for $H_2O$ are shown to be less than 5%, significantly lower than for other small molecules studied using this apparatus. Fragment ions formed *via* dissociative triple ionization are shown to comprise less than 0.1% of the total ion yield at 200 eV. Measurements of the KER involved in ion pair formation following dissociative double ionization of $H_2O$ reveal that indirect processes contribute significantly to the yield of $H^+ + OH^+$ ion pairs below the vertical double ionization threshold.

## Acknowledgement

The authors would like to acknowledge an EPSRC studentship for SJK.

## References

[1] D.E. Shemansky, D.T. Hall, J. Geophys. Res-Space Phys. 97 (1992) 4143.
[2] R.M. Haberli, M.R. Combi, T.I. Gombosi, D.L. De Zeeuw, K.G. Powell, Icarus 130 (1997) 373.
[3] B. Boudaiffa, P. Cloutier, D. Hunting, M.A. Huels, L. Sanche, Science 287 (2000) 1658.
[4] S.J. King, S.D. Price, J. Chem. Phys. 127 (2007) 174307.
[5] J. Schutten, F.J. Deheer, H.R. Moustafa, A.J. Boerboom, J Kistemak, J. Chem. Phys. 44 (1966) 3924.
[6] O.J. Orient, S.K. Srivastava, J. Phys. B: At. Mol. Opt. Phys. 20 (1987) 3923.
[7] M. Rao, I. Iga, S.K. Srivastava, J. Geophys. Res.-Planets 100 (1995) 26421.
[8] H.C. Straub, B.G. Lindsay, K.A. Smith, R.F. Stebbings, J. Chem. Phys. 108 (1998) 109.
[9] F. Frémont, C. Leclercq, A. Hajaji, A. Naja, P. Lemennais, S. Boulbain, V. Broquin, J.Y. Chesnel, Phys. Rev. A 72 (2005).
[10] E.C. Montenegro, S.W.J. Scully, J.A. Wyer, V. Senthil, M.B. Shah, J. Electron Spectrosc. Relat. Phenom. 155 (2007) 81.
[11] B. Siegmann, U. Werner, H.O. Lutz, R. Mann, J. Phys. B: At. Mol. Opt. Phys. 34 (2001) L587.
[12] U. Werner, K. Beckord, J. Becker, H.O. Lutz, Phys. Rev. Lett. 74 (1995) 1962.
[13] S.J. King, S.D. Price, Int. J. Mass Spectrom. 272 (2008) 154.
[14] P.J. Richardson, J.H.D. Eland, P.G. Fournier, D.L. Cooper, J. Chem. Phys. 84 (1986) 3189.
[15] D. Winkoun, G. Dujardin, L. Hellner, M.J. Besnard, J. Phys. B: At. Mol. Opt. Phys. 21 (1988) 1385.
[16] J.H.D. Eland, Chem. Phys. 323 (2006) 391.
[17] J.C. Severs, F.M. Harris, S.R. Andrews, D.E. Parry, Chem. Phys. 175 (1993) 467.
[18] W.E. Moddeman, T.A. Carlson, M.O. Krause, B.P. Pullen, W.E. Bull, G.K. Schweitz, J. Chem. Phys. 55 (1971) 2317.
[19] P.R. Bunker, O. Bludsky, P. Jensen, S.S. Wesolowski, T.J. Van Huis, Y. Yamaguchi, H.F. Schaefer, J. Mol. Spectrom. 198 (1999) 371.
[20] K. Nobusada, K. Tanaka, J. Chem. Phys. 112 (2000) 7437.
[21] T.J. Van Huis, S.S. Wesolowski, Y. Yamaguchi, H.F. Schaefer, J. Chem. Phys. 110 (1999) 11856.
[22] N.A. Love, S.D. Price, Phys. Chem. Chem. Phys. 6 (2004) 4558.
[23] D.M. Curtis, J.H.D. Eland, Int. J. Mass Spectrom. Ion Processes 63 (1985) 241.
[24] S. Harper, P. Calandra, S.D. Price, Phys. Chem. Chem. Phys. 3 (2001) 741.
[25] M.R. Bruce, R.A. Bonham, Int. J. Mass Spectrom. Ion Processes 123 (1993) 97.
[26] M.R. Bruce, L. Mi, C.R. Sporleder, R.A. Bonham, J. Phys. B: At. Mol. Opt. Phys. 27 (1994) 5773.
[27] C.S. O'Connor, S.D. Price, Int. J. Mass Spectrom. 184 (1999) 11.
[28] C.S.S. O'Connor, N. Tafadar, S.D. Price, J. Chem. Soc. -Faraday Trans. 94 (1998) 1797.
[29] T. Masuoka, E. Nakamura, A. Hiraya, J. Chem. Phys. 104 (1996) 6200.
[30] H.Y. Afeety, J.F. Liebman, S.E. Stein, Neutral Thermochemical Data, National Institute of Standards and Technology, Gaithersburg MD, June 2005, 20899 (http://webbook.nist.gov).
[31] S.G. Lias, NIST Chemistry WebBook, in: P.J. Linstrom, W.G. Mallard (Eds.), NIST Standard Reference Database Number 69, National Institute of Standards and Technology, Gaithersburg, MD, June 2005, 20899 (http://webbook.nist.gov).
[32] A.E. Slattery, T.A. Field, M. Ahmad, R.I. Hall, J. Lambourne, F. Penent, P. Lablanquie, J.H.D. Eland, J. Chem. Phys. 122 (2005).
[33] J.H.D. Eland, Mol. Phys. 61 (1987) 725.